JCI insight

RESEARCH ARTICLE

Pyruvate kinase M2 is requisite for Th1 and Th17 differentiation

Michihito Kono,[1,2] Kayaho Maeda,[1] Irina Stocton-Gavanescu,[1] Wenliang Pan,[1] Masataka Umeda,[1] Eri Katsuyama,[1] Catalina Burbano,[1] Seo Yeon K. Orite,[1] Milena Vukelic,[1] Maria G. Tsokos,[1] Nobuya Yoshida,[1] and George C. Tsokos[1]

[1]Department of Medicine, Beth Israel Deaconess Medical Center, Harvard Medical School, Boston Massachusetts, USA.
[2]Department of Rheumatology, Endocrinology and Nephrology, Faculty of Medicine, Hokkaido University, Sapporo, Japan.

Th1 and Th17 are important in the pathogenesis of autoimmune diseases and they depend on glycolysis as a source of energy. T cell antigen receptor signaling phosphorylates a serine/threonine kinase, calcium/calmodulin–dependent protein kinase IV (CaMK4), and promotes glycolysis. Based on these findings we hypothesized that CaMK4 promotes glycolysis. *Camk4*-deficient CD4$^+$ T cells and cells treated with a CaMK4 inhibitor had less glycolysis compared with their counterparts. Pull-down of CaMK4 and mass spectrometry identified pyruvate kinase muscle isozyme (PKM), the final rate-limiting enzyme in glycolysis, as a binding partner. Coimmunoprecipitation and Western blotting showed that CaMK4 interacts directly with PKM2. *Camk4*-deficient CD4$^+$ T cells displayed decreased pyruvate kinase activity. Silencing or pharmacological inhibition of PKM2 reduced glycolysis and in vitro differentiation to Th1 and Th17 cells, while PKM2 overexpression restored Th17 cell differentiation. Treatment with a PKM2 inhibitor ameliorated experimental autoimmune encephalomyelitis and CD4$^+$ T cells treated with PKM2 inhibitor or *Pkm2*-shRNA caused limited disease activity in an adoptive cell transfer model of experimental autoimmune encephalomyelitis. Our data demonstrate that CaMK4 binds to PKM2 and promotes its activity, which is requisite for Th1 and Th17 differentiation in vitro and in vivo. PKM2 represents a therapeutic target for T cell–dependent autoimmune diseases.

Introduction

Effector T helper cells, especially Th1 and Th17 cells, are important in the pathogenesis of autoimmune diseases including multiple sclerosis (MS), systemic lupus erythematosus (SLE), rheumatoid arthritis, and psoriasis (1–5). MS is a chronic inflammatory disease and demyelinating disease of the central nervous system (CNS) and autoreactive CD4$^+$ T cells with specificity for myelin antigens contribute to its pathogenesis (6, 7). Experimental autoimmune encephalomyelitis (EAE) is widely used to study the pathogenesis of MS in mice. SLE is a major autoimmune disease that affects multiple organs including the skin, kidney, and CNS. A complete understanding of the pathogenesis of SLE is still at large, while a diverse T cell effector dysfunction contributes to its expression (1).

Activated T cells including Th1 and Th17 cells utilize glycolysis to achieve the metabolic requirements for rapid proliferation and biosynthesis (8, 9). We have shown that pyruvate dehydrogenase phosphatase catalytic subunit 2 (PDP2), which promotes the activity of pyruvate dehydrogenase and facilitates entry into the oxidative phosphorylation circle from pyruvate, is reduced in Th17 cells from patients with SLE and that the overexpression of PDP2 reduced in vitro Th17 cell differentiation in MRL/*lpr* mice and patients with SLE (10). We have also shown that Th17 cells depend on glutaminolysis more than the other T cell subsets and glutaminase 1, the first enzyme in glutaminolysis, is upregulated in Th17 cells (11) and an inhibitor of glutaminase 1 reduced the disease activity in EAE (11). These findings suggest that cell metabolism can be targeted therapeutically in autoimmune diseases.

Calcium/calmodulin–dependent protein kinase IV (CaMK4) is a multifunctional serine/threonine kinase that regulates the expression of several genes (12–14). Previously, we have shown that CaMK4 is increased in the nuclei of T cells from patients with SLE (15) and is necessary for Th17 differentiation (13). *Camk4*-deficient MRL/*lpr* mice and mice treated with an inhibitor of CaMK4 have reduced autoantibody production and proteinuria (16, 17). Moreover, *Camk4*-deficient mice and mice treated with an inhibitor of CaMK4 have less EAE

Authorship note: NY and GCT contributed equally to this work.

Conflict of interest: The authors have declared that no conflict of interest exists.

Submitted: January 11, 2019
Accepted: May 16, 2019
Published: June 20, 2019.

Reference information: *JCI Insight*. 2019;4(12):e127395. https://doi.org/10.1172/jci.insight.127395.

disease activity (13). However, we do not know how CaMK4 affects T cell function. T cell antigen receptor (TCR) signaling triggers production of the second messengers Ca^{2+} and phosphorylates CaMK4. Cell metabolism is central to T cell differentiation and Th17 cells are known to use mainly glycolysis (18, 19). Because TCR signaling induces rapid aerobic glycolysis in minutes to hours (20), we hypothesized that CaMK4 promotes glycolysis in a direct manner by controlling the activity of the involved metabolic enzymes.

Pyruvate kinase is at the final step of glycolysis and converts phosphoenolpyruvate to pyruvate. Pyruvate kinase has 4 isozymes: L (liver), R (erythrocytes), M1 (muscles, hearts and brain), and M2 (early fetal tissue, lung, fat tissue, many tumor cells, and other cells). Pyruvate kinase muscle isozyme 1 (PKM1) and PKM2 are different splicing variants of the *Pkm* gene (exon 9 for PKM1 and exon 10 for PKM2).

Here, we report that CaMK4 binds PKM2 and promotes pyruvate kinase activity. PKM2 is requisite for Th1 and Th17 cell differentiation and its silencing or pharmacologic inhibition reduces disease activity in EAE. Our data demonstrate that inhibition of PKM2 is a potential treatment option for T cell–dependent autoimmune diseases.

Results

CaMK4 promotes glycolysis. Previous studies have shown that the activity of CaMK4 is regulated mainly by phosphorylation and calcium and calmodulin are needed for the phosphorylation of CaMK4 (12). Ionomycin is an effective Ca^{2+} ionophore and increases intracellular calcium levels and leads to the phosphorylation of CaMK4 within 5 minutes (21). To examine how activated CaMK4 affects glycolysis, we examined glycolysis in *Camk4*-sufficient or -deficient $CD4^+$ T cells in the presence or absence of ionomycin.

Naive $CD4^+$ T cells were purified from spleens of *Camk4*-sufficient or -deficient mice and stimulated with anti-CD3 and -CD28 Abs for 36 hours in vitro and extracellular acidification rate (ECAR) was analyzed by an extracellular flux analyzer. DMSO or ionomycin was added during the glycolysis stress test with acute injection (Supplemental Figure 1; supplemental material available online with this article; https://doi.org/10.1172/jci.insight.127395DS1). Although glycolysis and glycolytic capacity were not significantly different from these groups in the absence of ionomycin, glycolysis and glycolytic capacity in T cells from *Camk4*-deficient mice were significantly decreased in the presence of ionomycin compared with those from *Camk4*-sufficient mice (Figure 1, A and B). To confirm these observations, naive $CD4^+$ T cells were purified from spleens of *Camk4*-sufficient mice and stimulated with CD3 and CD28 Abs for 36 hours, and ECAR was measured after 1 hour of pretreatment with the CaMK4 inhibitor KN-93. One-hour pretreatment of cells with KN-93 resulted in decreased glycolysis and glycolytic capacity under ionomycin stimulation (Figure 1, C and D). These data indicate that CaMK4 promotes glycolysis in the presence of ionomycin.

Because we have previously shown that CaMK4 is increased in Th17, but not Th1 cells, and is requisite for Th17 differentiation but not for Th1 differentiation, we examined the ECAR under Th1- or Th17-polarizing conditions with ionomycin stimulation in *Camk4*-sufficient or -deficient T cells. As we expected, glycolysis and glycolytic capacity in T cells from *Camk4*-deficient mice under Th17-polarizing conditions were significantly decreased compared with those from *Camk4*-sufficient mice, but not under Th1-polarizing conditions (Figure 1, E–H).

CaMK4 binds to PKM2 and activates pyruvate kinase activity. To examine how CaMK4 promotes glycolysis, we performed a pull-down assay with Flag-tagged human CaMK4 (hCaMK4) followed by mass spectrometry (MS). HEK293T cells were transfected with Flag-tagged hCaMK4 and a pull-down assay was performed using an anti-Flag Ab. Candidate proteins binding to CaMK4 protein determined by MS are listed in Table 1. Out of 32 proteins, PKM and ATP-dependent 6-phosphofructokinase, platelet type (PFKP) are components of the glycolytic pathway (Table 1). ATP-dependent 6-phosphofructokinase (PFK) is a rate-limiting enzyme of glycolysis and irreversibly converts fructose 6-phosphate to fructose 1,6-bisphosphate. PFK has 3 types of subunits: PFKM (muscle type), PFKL (liver type), and PFKP (platelet type). Pyruvate kinase is at the final step of glycolysis and converts phosphoenolpyruvate to pyruvate. Fructose 1,6-bisphosphate, which is converted from fructose 6-phosphate by PFK, is an allosteric activator of pyruvate kinase (Supplemental Figure 2). PKM1 and PKM2 are different splicing variants of the *Pkm* gene. From the distribution of these isozymes in T cells (22), we focused on PKM2.

To confirm whether CaMK4 binds to PKM2, HEK293T cells were transfected with Flag-hCaMK4 and 6×His-tagged human PKM2 (hPKM2) or 6×His-tagged enhanced green fluorescent protein (EGFP), followed by coimmunoprecipitation (Co-IP) using Flag or 6×His Abs. The 6×His-tagged EGFP was used to rule out possible nonspecific interaction between 6×His-tagged and FLAG-tagged proteins. Co-IP and

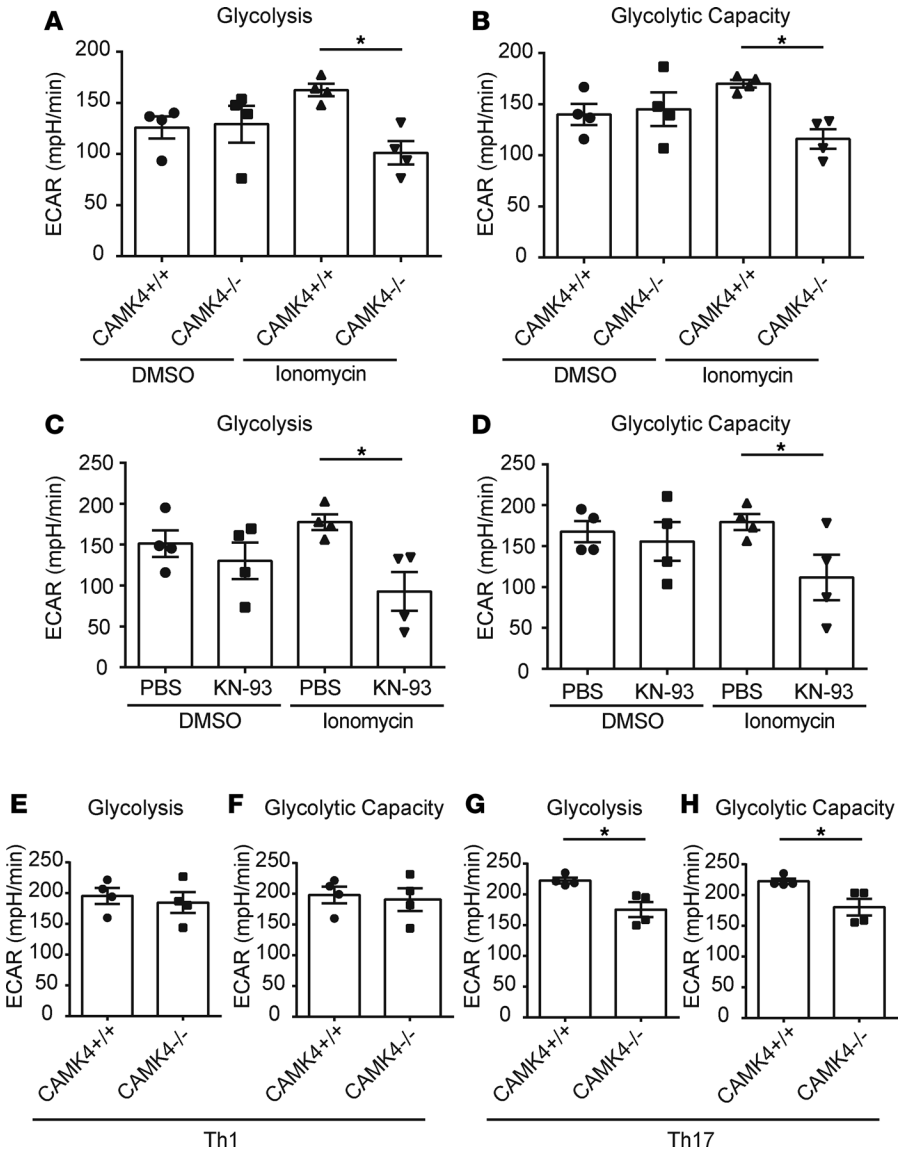

Figure 1. CaMK4 promotes glycolysis under ionomycin stimulation. (**A** and **B**) *Camk4*-sufficient or -deficient naive CD4$^+$ T cells were cultured with CD3 and CD28 Abs for 36 hours in vitro and extracellular acidification rate (ECAR) was analyzed by an extracellular flux analyzer. Glycolysis (**A**) and glycolytic capacity (**B**) in T cells from *Camk4*-sufficient or -deficient mice with or without ionomycin stimulation. Cumulative data of ECAR are shown (mean ± SEM); n = 4. (**C** and **D**) *Camk4*-sufficient naive CD4$^+$ T cells were cultured with CD3 and CD28 Abs for 36 hours and after 1-hour pretreatment with or without CaMK4 inhibitor, KN-93, ECAR was measured. Glycolysis (**C**) and glycolytic capacity (**D**) in T cells with or without KN-93 (n = 4). Cumulative data of ECAR are shown (mean ± SEM); n = 4. *P < 0.05 by ANOVA. (**E**–**H**) *Camk4*-sufficient or -deficient naive CD4$^+$ T cells were cultured under Th1- (**E** and **F**) or Th17-polarizing conditions (**G** and **H**) for 3 days in vitro and ECAR was analyzed by an extracellular flux analyzer. Glycolysis (**E** and **G**) and glycolytic capacity (**F** and **H**) in T cells from *Camk4*-sufficient or -deficient mice with ionomycin stimulation. Cumulative data of ECAR are shown (mean ± SEM); n = 4. *P < 0.05 by 2-tailed t test.

Western blotting in these cells showed that CaMK4 directly interacted with PKM2 (Figure 2, A and B).

Furthermore, we performed Co-IP and Western blotting using primary T cells. *Camk4*-deficient naive CD4$^+$ T cells were transfected with Flag-tagged mouse CaMK4 (mCaMK4) under Th17-polarizing conditions, followed by Co-IP using Flag or IgG Abs. Western blotting was performed using PKM2 Ab. The results of this experiment showed that CaMK4 directly interacts with PKM2 in Th17-polarized primary T cells (Figure 2C).

To clarify whether CaMK4 controls pyruvate kinase activity, *Camk4*-sufficient or -deficient naive CD4$^+$ T cells were cultured with CD3 and CD28 Abs for 48 hours in vitro and after 2-hour pretreatment with ionomycin, cells were collected and pyruvate kinase activity was measured. *Camk4*-deficient CD4$^+$ T cells

Table 1. Candidate proteins binding to CaMK4 protein identified by mass spectrometry

Candidate proteins by mass spectrometry
N-α-acetyltransferase 15, NatA auxiliary subunit
Dolichyl-diphosphooligosaccharide--protein glycosyltransferase subunit 1
T-complex protein 1 subunit γ
Trifunctional enzyme subunit α, mitochondrial
Heat shock protein 75 kDa, mitochondrial
78 kDa glucose-regulated protein
Glycogen phosphorylase, brain form
ATP-binding cassette subfamily E member 1
Far upstream element–binding protein 2
Isoform 2 of signal recognition particle subunit SRP72
Nuclear pore complex protein Nup93
Pyruvate kinase muscle isozyme, PKM
Insulin-like growth factor 2 mRNA-binding protein 2
Cleavage and polyadenylation-specificity factor subunit 6
26S proteasome non-ATPase regulatory subunit 2
Helicase SKI2W
Melanoma-associated antigen D2
Isoform 2 of ATP synthase subunit α, mitochondrial
Tubulin--tyrosine ligase–like protein 12
Vesicle-fusing ATPase
Calpain-2 catalytic subunit
Glycine--tRNA ligase
Isoform 3 of pre-mRNA 3′-end–processing factor FIP1
Pentatricopeptide repeat domain–containing protein 3, mitochondrial
Isoform 2 of ATP-binding cassette subfamily F member 2
Ras GTPase-activating–like protein IQGAP2
ATP-dependent 6-phosphofructokinase, platelet type
Calpain-1 catalytic subunit
Isoform CNPI of 2′,3′-cyclic-nucleotide 3′-phosphodiesterase
Guanine nucleotide–binding protein–like 1
Isoform mitochondrial of lysine--tRNA ligase
Isoform 2 of NF-κ-B–repressing factor

had reduced pyruvate kinase activity compared with their counterparts (Figure 2D). From these data we conclude that CaMK4 binds to PKM2 and enhances its activity.

PKM2 promotes in vitro Th1 and Th17 cell differentiation. To examine whether PKM2 is important in T cell differentiation, naive $CD4^+$ T cells were cultured under Th1-, Th17-, or Treg-polarizing conditions with or without the PKM2 inhibitor shikonin, which reduces pyruvate kinase activity (23). ECAR was measured in Th1, Th17, and Treg cells in the presence or absence of shikonin. The presence of shikonin reduced glycolysis and glycolytic capacity in Th1 and Th17 cells (Figure 3, A and B) but it did not reduce glycolysis in Treg cells (Supplemental Figure 3A).

Shikonin reduced the percentages of IFN-γ–producing (Figure 3, C and D) and IL-17A–producing (Figure 3, E and F) $CD4^+$ T cells in a dose-dependent manner, but at low concentrations it did not reduce the percentages of $CD4^+CD25^+Foxp3^+$ T cells (Supplemental Figure 3, B and C). The ratios of the percentage in each T cell subset with shikonin versus those without shikonin were significantly reduced in Th1 and Th17 compared with Treg cells (Supplemental Figure 3D). Because one group has recently shown that PKM2 is important in the hyperhomocysteinemia-promoted IFN-γ secretion by $CD4^+$ T cells in hyperhomocysteinemia-accelerated atherosclerosis (22), we focused on the importance of PKM2 in Th17 cells.

To confirm the effect of PKM2 inhibition on Th17-polarized T cells, 2 different *Pkm2*-specific shRNAs were generated. After confirming that *Pkm2*-specific shRNA reduced PKM2 protein levels (Figure 3, G and H), naive $CD4^+$ T cells were cultured under Th17-polarizing conditions and transfected with *Pkm2*-specific shRNA or control shRNA. The percentage of IL-17A–producing $CD4^+$ T cells was significantly reduced

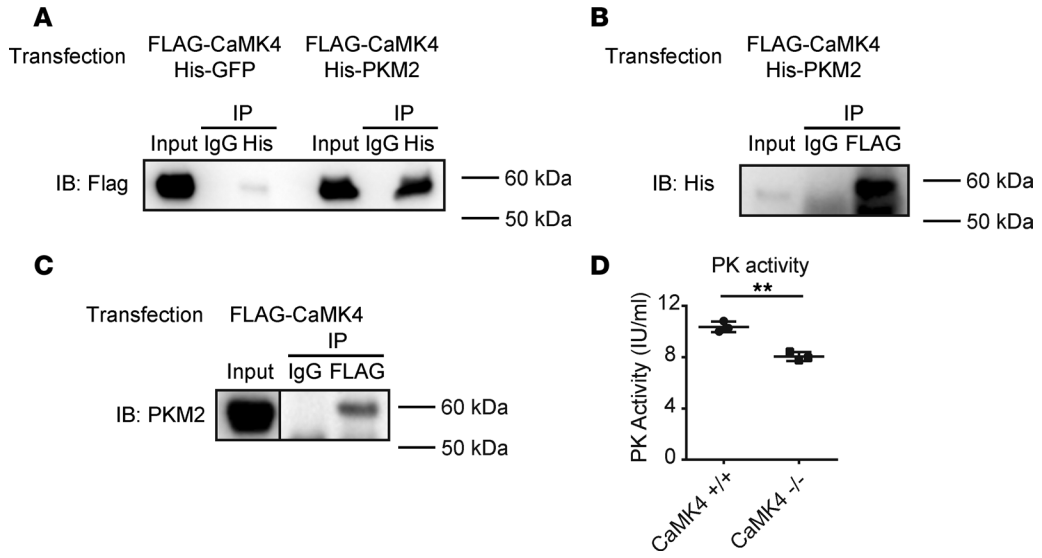

Figure 2. CaMK4 binds to PKM2 and increases pyruvate kinase activity. (**A** and **B**) HEK293T cells were transfected with Flag-hCaMK4 and 6×His-hPKM2 or 6×His-tagged enhanced green fluorescent protein (His-EGFP), followed by coimmunoprecipitation using anti-Flag, anti-6×His, or anti–mouse IgG Abs. Western blotting was performed using anti-Flag (**A**) or 6×His (**B**) Abs. Data are representative of 3 independent experiments. (**C**) *Camk4*-deficient naive CD4$^+$ T cells were transfected with Flag-mCaMK4 under Th17-polarizing conditions, followed by coimmunoprecipitation using Flag or mouse IgG Abs. Western blotting was performed using PKM2 Ab. Data are representative of 2 independent experiments. (**D**) *Camk4*-sufficient or -deficient naive CD4$^+$ T cells were cultured with CD3 and CD28 Abs for 48 hours in vitro and after 2-hour pretreatment with ionomycin, cells were collected and pyruvate kinase activity was measured. Cumulative data are shown (mean ± SEM); $n = 3$. $^{**}P < 0.01$ by 2-tailed t test. IB, immunoblotting; IP, immunoprecipitation.

in *Pkm2*-specific shRNA–treated T cells compared with the control shRNA–treated group (Figure 3I). Furthermore, we generated a mouse PKM2 (mPKM2) vector using the pIRES2-DsRed-Express vector (Supplemental Figure 3E). Naive CD4$^+$ T cells were cultured under Th17- or Treg-polarizing conditions and transfected with empty or mPKM2 vector. PKM2 overexpression increased Th17 cell differentiation but not Treg differentiation (Figure 3J and Supplemental Figure 3, F–H). These data confirmed that PKM2 is crucial for Th17 cell differentiation.

To evaluate the effect of shikonin on cell viability, 7AAD$^+$annexin V$^+$ cells and 7AAD$^-$annexin V$^+$ cells were measured in Th1-, Th17-, and Treg-polarized cells with various concentrations of shikonin on day 3. Shikonin did not change the proportion of 7AAD$^+$annexin V$^+$ cells or 7AAD$^-$annexin V$^+$ cells (Supplemental Figure 4, A–F), suggesting that the effects of shikonin are not due to changes in cell viability. The same cells were evaluated by flow cytometry using Ki67 as a proliferation marker. Because shikonin did not change the proportion of Ki67$^+$ cells in vitro (Supplemental Figure 4, G–I), the reduction of Th1- and Th17-polarized cells was not due to cell cycle disruption but to inhibition of differentiation. Furthermore, as a T cell activation marker, CD44$^+$ cells were analyzed by flow cytometry (Supplemental Figure 4, J–L). Shikonin did not change the proportion of CD44$^+$ cells on day 3, suggesting that shikonin does not simply inhibit T cell activation but also inhibits Th1 and Th17 cell differentiation.

PKM2 inhibitor ameliorates EAE. To examine whether PKM2 is a therapeutic target for autoimmune diseases we subjected B6 mice to EAE and treated them with shikonin or DMSO. Treatment of mice with shikonin significantly reduced both the clinical score (Figure 4A) and body weight loss (Figure 4B) compared with treatment with DMSO. Histology scores of spinal cords from diseased animals were significantly decreased in the shikonin-treated group (Figure 4, C and D). This observation was further confirmed by assessing the absolute numbers of spinal cord–infiltrating cells by flow cytometry. Treatment with shikonin reduced the numbers of CD4$^+$ T cells (Figure 4E), IFN-γ–producing (Figure 4F), and IL-17A–producing CD4$^+$ T cells (Figure 4G) in the spinal cord compared with those of animals treated with DMSO.

PKM2 inhibitor–treated CD4$^+$ T cells cause reduced disease activity in an adoptive cell transfer EAE model. To clarify whether the effect of shikonin on EAE is T cell dependent or not, an adoptive cell transfer EAE experiment was performed. CD4$^+$ T cells from 2D2 mice, which express a myelin oligodendrocyte

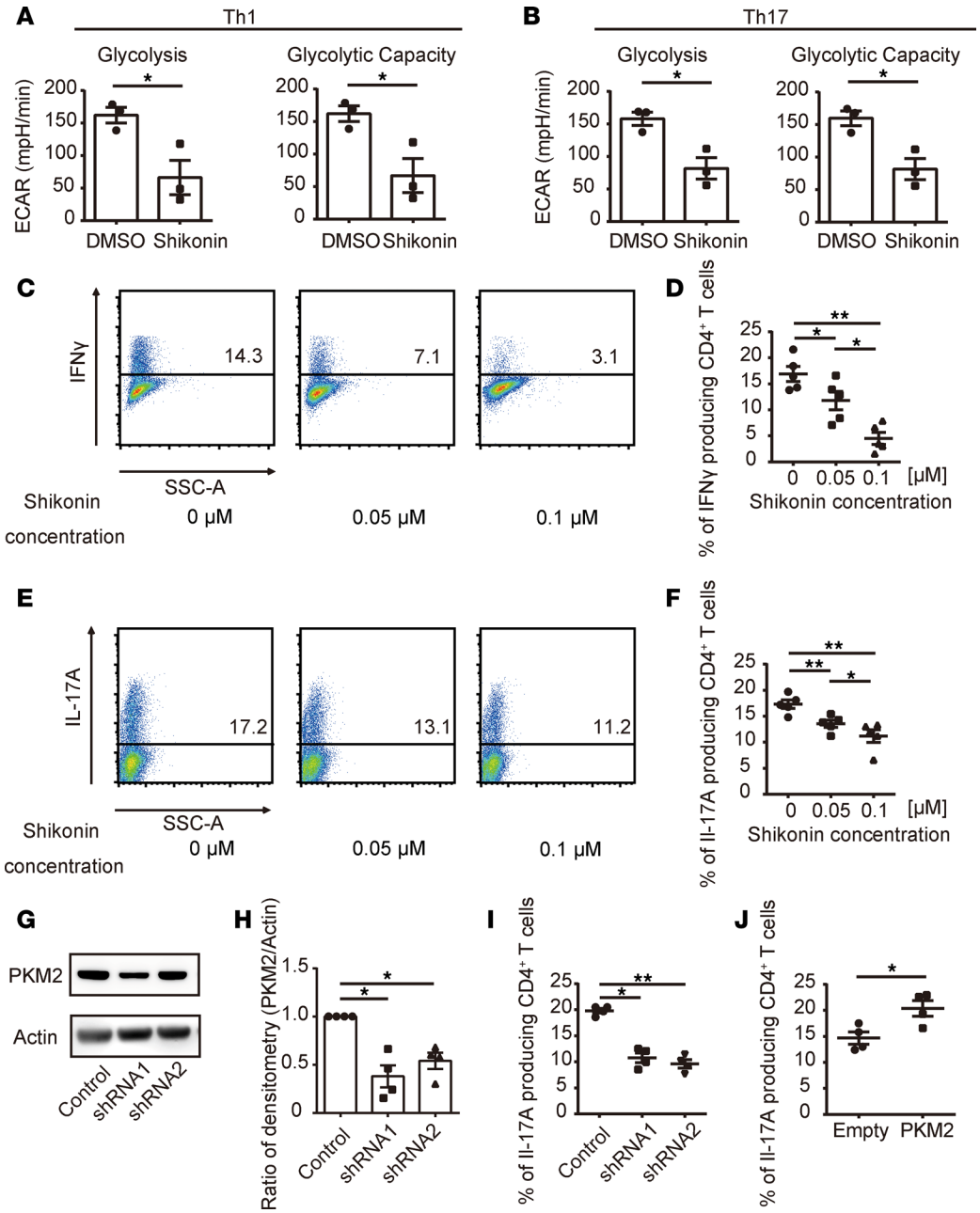

Figure 3. PKM2 promotes in vitro Th1 and Th17 differentiation. (**A**–**F**) Naive CD4$^+$ T cells were cultured for 3 days under Th1- and Th17-polarizing conditions and various concentration of shikonin were added on day 0. (**A** and **B**) Extracellular acidification rate (ECAR) in Th1 (**A**) and Th17 cells (**B**) with or without shikonin was measured on day 3. Cumulative data are shown (mean ± SEM); $n = 3$. (**C** and **E**) Representative flow plots of IFN-γ–producing (**C**) and IL-17A–producing (**E**) CD4$^+$ T cells are shown. (**D** and **F**) Cumulative data of IFN-γ–producing (**D**) and IL-17A–producing (**F**) CD4$^+$ T cells are shown (mean ± SEM); $n = 5$. (**G**–**I**) Naive CD4$^+$ T cells were cultured for 4 days under Th17-polarizing conditions and transfected with control shRNA or *Pkm2*-specific shRNA on day 1. (**G**) PKM2 and actin protein expression on day 3 was assessed by Western blotting. Representative blots are shown. Data are representative of 4 experiments. (**H**) Cumulative data of the Western blotting densitometric ratio (PKM2/actin) are shown (mean ± SEM); $n = 4$. (**I**) Cumulative data of flow plots of IL-17A–producing CD4$^+$ T cells are shown (mean ± SEM); $n = 4$. (**J**) Naive CD4$^+$ T cells were cultured for 3 days under Th17-polarizing conditions and transfected with empty vector or mouse PKM2–expressing vector on day 1. Cumulative data of IL-17A–producing CD4$^+$ T cells are shown (mean ± SEM); $n = 4$. $^*P < 0.05$; $^{**}P < 0.01$ by 2-tailed t test (**A**, **B**, and **J**) or 1-way ANOVA with Bonferroni's multiple-comparisons test (**D**, **F**, **H**, and **I**).

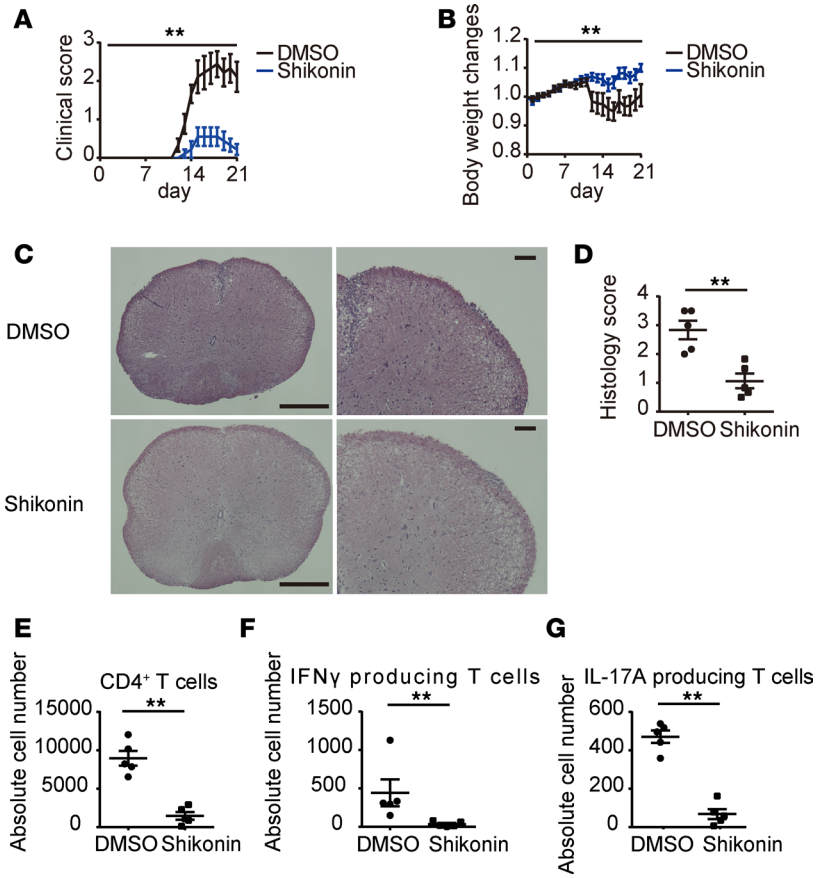

Figure 4. PKM2 inhibitor ameliorates EAE. (**A**–**G**) EAE was induced in B6 mice by immunization with MOG35-55 emulsified in complete Freund's adjuvant. Mice were treated with DMSO or shikonin twice a week intraperitoneally. (**A**) Clinical scores. (**B**) Body weight changes. Cumulative results of 2 independent experiments with 5 mice per group are shown (mean ± SEM); $n = 10$. (**C** and **D**) Spinal cords were harvested on day 14 and stained with H&E to evaluate inflammation. (**C**) Representative images show H&E staining of spine from DMSO- or shikonin-treated mice. Scale bars: 500 μm or 100 μm (higher-magnification images on right). (**D**) Quantitative cumulative data are shown (mean ± SEM); $n = 5$. (**E**–**G**) Absolute cell numbers of spinal cord–infiltrating $CD4^+$ T cells (**E**), IFN-γ–producing (**F**), and IL-17A–producing $CD4^+$ T cells (**G**) from DMSO- or shikonin-treated mice were evaluated by flow cytometry on day 14. Cumulative data are shown (mean ± SEM); $n = 5$. $^{**}P < 0.01$ by 2-way ANOVA (**A** and **B**) or 2-tailed *t* test (**D**–**G**).

glycoprotein (MOG) TCR, were cultured with MOG35-55, mitomycin-treated splenocytes, and rIL-12 for 48 hours and DMSO or shikonin was added on day zero. The percentages of IFN-γ– and IL-17A–producing cells were reduced in shikonin-treated $CD4^+$ T cells compared with DMSO-treated cells (Supplemental Figure 5, A and B). These cells were also transferred into *Rag1*-deficient mice. The mice that received PKM2 inhibitor–treated 2D2 T cells had reduced clinical scores (Figure 5A) and body weight loss (Figure 5B) compared with the control group. Histology scores of spinal cords from diseased animals were significantly decreased in the mice that received shikonin-treated cells (Figure 5, C and D). Absolute cell numbers of spinal cord–infiltrating cells were assessed by flow cytometry. IFN-γ–producing (Figure 5E) and IL-17A–producing (Figure 5F) cells were reduced in the mice that received shikonin-treated cells compared with their control-treated counterparts. These results confirmed that shikonin ameliorates EAE in a T cell–dependent manner.

Pkm2-shRNA–transfected Th17 cells cause reduced disease activity in an adoptive cell transfer EAE model. To confirm the requisite role of PKM2 in Th17 in vivo, another adoptive cell transfer EAE experiment was performed. Naive $CD4^+$ T cells from 2D2 mice were cultured under Th17-polarizing conditions and transfected with *Pkm2*-shRNA or control shRNA and transferred into *Rag1*-deficient mice. The mice that received *Pkm2*-shRNA–transfected 2D2 T cells exhibited reduced EAE disease activity compared with those that received cells transfected with control shRNA (Figure 6, A and B). To confirm

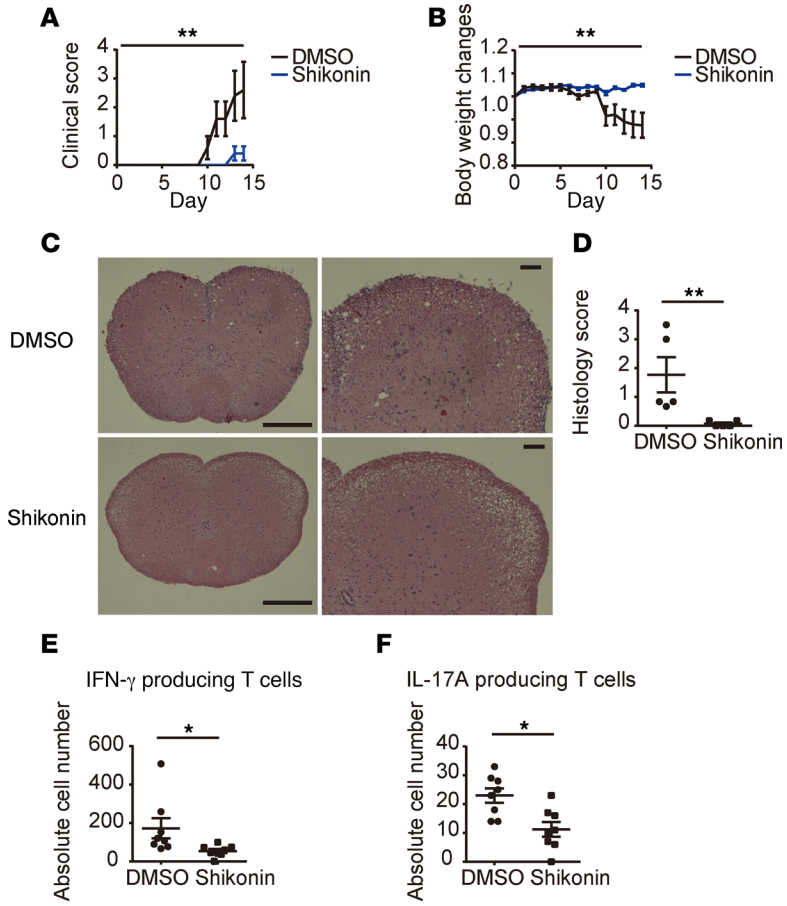

Figure 5. PKM2 inhibitor–treated CD4⁺ T cells ameliorate disease activity in an adoptive cell transfer EAE model. (**A**–**D**) CD4⁺ T cells from 2D2 mice were cultured with 20 μg/ml MOG35-55, mitomycin-treated splenocytes, and 0.5 ng/ml rIL-12 for 48 hours and DMSO or shikonin was added on day 0. On day 2, these cells were transferred into *Rag1*-deficient mice intravenously and EAE was induced. (**A** and **B**) Clinical scores (**A**) and body weight changes (**B**) of recipient mice are shown. Cumulative results are shown (mean ± SEM); $n = 5$. (**C** and **D**) Spinal cords were harvested on day 14 and stained with H&E to evaluate inflammation. (**C**) Representative images show H&E staining of spine from the mice that received DMSO- or shikonin-treated cells. Scale bars: 500 μm or 100 μm (higher-magnification images on right). (**D**) Quantitative cumulative data are shown (mean ± SEM); $n = 5$. (**E** and **F**) Absolute cell numbers of spinal cord–infiltrating IFN-γ–producing (**E**) and IL-17A–producing CD4⁺ T cells (**F**) from the mice that received DMSO- or shikonin-treated cells were evaluated by flow cytometry on day 14. Cumulative data are shown (mean ± SEM); $n = 8$. $^*P < 0.05$. $^{**}P < 0.01$ by 2-way ANOVA (**A** and **B**) or 2-tailed t test (**D**–**F**).

these data, the absolute numbers of spinal cord–infiltrating cells were examined by flow cytometry. *Rag1*-deficient mice that received *Pkm2*-shRNA–transfected 2D2 T cells had decreased numbers of IL-17A–producing CD4⁺ T cells in the spinal cord compared with those that received cells transfected with control shRNA (Figure 6C).

Discussion

In this study, we demonstrate that PKM2 is requisite for Th1 and Th17 differentiation and PKM2 can serve as a therapeutic target for T cell–dependent autoimmune diseases. Mechanistically, the serine/threonine kinase CaMK4 binds PKM2 and promotes its activity and glycolysis.

Th1 and Th17 cells are significant in the expression of autoimmune diseases including MS, SLE, rheumatoid arthritis, and psoriasis (1–4). Although a number of treatment modalities including corticosteroids, immunosuppressants, and biologic agents have been introduced in the treatment of these entities, severe and/or refractory cases are often encountered that require additional considerations. Furthermore, many patients with autoimmune diseases suffer side effects when treated with the available medications emphasizing the importance of the need for new approaches.

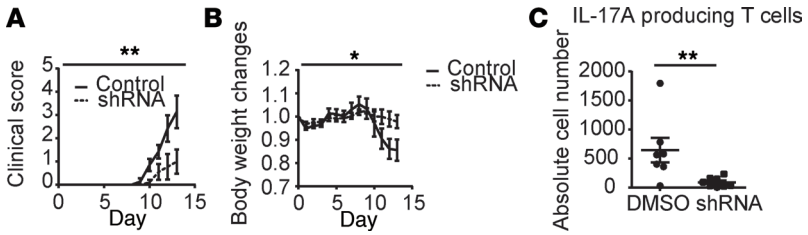

Figure 6. *Pkm2*-shRNA–transfected Th17 cells reduce disease activity in an adoptive cell transfer EAE model. (**A**–**C**) Naive CD4$^+$ T cells from 2D2 mice were cultured under Th17-polarizing conditions and transfected with *Pkm2*-shRNA or control shRNA. These cells were transferred into *Rag1*-deficient mice intravenously and EAE was induced. (**A**) Clinical scores of recipient mice are shown. Cumulative results of 2 independent experiments with 3–4 mice per group are shown (mean ± SEM); n = 7–8. (**B**) Cumulative results of body weight changes of recipient mice (mean ± SEM); n = 7–8. (**C**) Spinal cords were harvested on day 14, and absolute cell numbers of spinal cord–infiltrating IL-17A–producing CD4$^+$ T cells from the mice that received *Pkm2*-specific– or control shRNA–treated cells were evaluated by flow cytometry on day 14. Cumulative data are shown (mean ± SEM); n = 7–8. $^*P < 0.05$; $^{**}P < 0.01$ by 2-way ANOVA (**A** and **B**) or 2-tailed t test (**C**).

Cell metabolism is important in T cell differentiation (18, 19) and Th1 and Th17 cells use mainly glycolysis, whereas Treg cells use fatty acid oxidation (19). Activation of mechanistic target of rapamycin complex 1 (mTORC1) promotes glycolysis in Th1 and Th17 cells (24, 25). Glycolysis is requisite for proliferating cells because glycolysis produces energy quickly compared with that produced by the tricarboxylic acid cycle (8) and enables the generation of materials to produce DNA, RNA, proteins, and lipids. Because cell metabolism regulates T cell fate, modulation of metabolic pathways had been considered as a source for novel therapeutic targets (26–28).

PKM2 is the final rate-limiting enzyme in glycolysis and catalyzes the conversion of phosphoenolpyruvate to pyruvate and is upregulated in tumor cells. Although PKM2 has been mainly studied in the oncology field (29), few reports have considered the role of PKM2 in T cells (22). One group has recently shown that PKM2 is important for hyperhomocysteinemia-promoted IFN-γ production from CD4$^+$ T cells in hyperhomocysteinemia-accelerated atherosclerosis (22), while the role of PKM2 in T cells in autoimmune diseases is still unclear. Our data demonstrate that PKM2 has a crucial role in Th1 and also Th17 differentiation and that PKM2 could be a potential target for the treatment of T cell–dependent autoimmune disease.

We have previously demonstrated that the serine/threonine kinase CaMK4 promotes mTORC1 activity and is crucial for Th17 differentiation. CaMK4 accelerates disease activity in EAE and lupus-prone mice. Our data demonstrate that glycolysis in *Camk4*-deficient CD4$^+$ T cells is reduced compared with their counterparts. The CaMK4 inhibitor KN-93 prevents the activation of CaMK4 and reduced glycolysis after ionomycin stimulation. Furthermore, we demonstrated that CaMK4 binds PKM2 and increases its activity and glycolysis. It is possible that CaMK4 affects glycolysis at additional points including the expression of glucose transporter 1 (GLUT-1), which was reportedly decreased in KN-93–treated Th17-polarized cells from patients with SLE (30). Because silencing of PKM2 reduces the expression of GLUT-1 in a gastric cancer cell line (31) and chondrocytes (32), KN-93 may have reduced GLUT-1 expression through PKM2 in T cells.

We have previously shown that CaMK4 is increased in Th17 but not Th1 cells and is requisite for Th17 differentiation and is not for Th1 differentiation (13). Glycolysis in T cells from *Camk4*-deficient mice under Th17-polarizing conditions was significantly decreased compared with those from *Camk4*-sufficient mice, but not under Th1-polarizing conditions. PKM2 is requisite for both Th1 and Th17 cell differentiation, suggesting another mechanism that enhances PKM2 in Th1 cells.

In summary, we have shown that PKM2 is requisite for Th1 and Th17 differentiation and that silencing and pharmacological inhibition of PKM2 reduces the activity of EAE in a T cell– and Th17-dependent manner. Mechanistically, the serine/threonine kinase CaMK4 binds PKM2 and stimulates pyruvate kinase activity and promotes glycolysis. These data present potentially new mechanisms in cellular metabolism in Th1 and Th17 cells and suggest new therapeutic targets for T cell–dependent autoimmune diseases.

Methods

Mice. B6.129X1-Camk4tm1Tch/J, C57BL/6-Il17atm1Bcgen/J (IL-17GFP), C57BL/6-Tg(Tcra2D2, Tcrb-2D2)1Kuch/J (2D2), MRL/MpJ-Faslpr/J (MRL/*lpr*), and B6.129S7-Rag1tm1Mom/J (*Rag1*-KO) mice were purchased from The Jackson Laboratory. B6.IL-17GFP mice were made by crossing B6 mice with IL-17GFP mice. Animals were sacrificed at the end of their 8–12 weeks of life for in vitro culture experiments and on the indicated week for in vivo experiments. All mice were maintained in a specific pathogen–free animal facility (Beth Israel Deaconess Medical Center).

Single-cell isolation. For mouse, spleen and lymph node lymphocytes as well as infiltrating lymphocytes in spinal cords were isolated as previously described (11).

In vitro T cell differentiation. Naive $CD4^+$ T cells were purified by mouse $CD4^+CD62L^+$ T Cell Isolation Kit II (Miltenyi Biotec). Purified naive T cells were stimulated with plate-bound goat anti-hamster Abs, soluble anti-CD3 (0.25 μg/ml, 145-2C11; Biolegend), and anti-CD28 (0.5 μg/ml, 37.51; Biolegend) for Th0-nonpolarizing condition culture. In addition to Th0-nonpolarizing conditions, the following stimulation protocols were used for each polarizing condition: IL-12 (20 ng/ml; R&D Systems) and anti-IL-4 (10 μg/ml, C17.8; Biolegend) for Th1; IL-6 (10 ng/ml; R&D Systems), TGF-β1 (0.3 ng/ml; R&D Systems), anti–IL-4 (10 μg/ml, C17.8; Biolegend), and anti–IFN-γ (10 μg/ml; XMG1.2; Biolegend) for Th17; IL-2 (20 ng/ml; R&D Systems), TGF-β1 (3 ng/ml; R&D Systems), anti–IL-4 (10 μg/ml, C17.8; Biolegend), and anti–IFN-γ (10 μg/ml, XMG1.2; Biolegend) for Treg (11). For the PKM2 inhibition, shikonin (0.1 μM or indicated concentration; Sigma-Aldrich) dissolved in DMSO or the same concentration of DMSO was added to cultures on day 0.

Metabolism assays. ECAR was measured using an XFp extracellular flux analyzer. All other procedures were performed according to the manufacturer's instructions as previously described (10). Ionomycin (1 μM) dissolved in DMSO or the same concentration of DMSO was added during the glycolysis stress test with acute injection (Supplemental Figure 1).

Western blotting. Cell lysates ware separated in a NuPAGE 4%–12% Bis-Tris gel (Life Technologies) and proteins were transferred to a nitrocellulose membrane. The following Abs were used: anti-Flag (M2, Sigma-Aldrich); anti-actin (AC-74, Sigma-Aldrich); anti–His tag (27E8, Cell Signaling Technology); anti-PKM2 (D78A4, Cell Signaling Technology); goat anti–mouse IgG coupled with HRP and goat anti–rabbit IgG coupled with HRP (Jackson ImmunoResearch). The ECL system (Amersham) was used for detection. Bands on blots corresponding to proteins of interest were analyzed by ImageJ software (NIH).

Flow cytometry. The following Abs purchased from BioLegend were used for flow cytometry analysis: mouse CD4 (GK1.5), CD8a (53-6.7), CD25 (PC61), CD44 (IM7), CD45 (30-F11), CD90.2 (53-2.1), Ki67 (16A8), IL-17A (JC11-18H10.1), and IFN-γ (XMG1.2). CD3α (17A2) and Foxp3 (FJK-16s) Abs were purchased from eBioscience. 7AAD, annexin V (surface), or a Zombie Aqua Fixable Viability Kit (intracellular) staining was performed for eliminating dead cells. Surface staining was performed on ice for 20–30 minutes. Absolute cell numbers were calculated based on the percentage of each cell population. For intracellular staining, harvested cells were stimulated for 4 hours in culture medium with PMA (Sigma-Aldrich), ionomycin (Sigma-Aldrich), and monensin (BD Biosciences). Cytofix/Cytoperm and Perm/Wash buffer (Ki67/IL-17A/IFN-γ; BD Biosciences) or Mouse Regulatory T Cell Staining Kit (Foxp3; eBioscience) was used for fixation and permeabilization. All flow cytometry data were acquired on a BD LSRII (BD Biosciences) or Cytoflex LX (Beckman Coulter) and analyzed with FlowJo (FlowJo, LLC). All procedures were performed according to the manufacturer's instructions. For mPKM2 overexpression experiments under Th17-polarized conditions in murine primary T cells, IL-17GFP mice were used. For mPKM2 overexpression experiments under Treg-polarizing conditions, Zombie Aqua–$DsRed^+$ cells were sorted by FACSAria II cell sorter (BD Biosciences) and stained for CD25, followed by Foxp3 staining as described above.

Enzyme activity. Pyruvate kinase enzyme activity on day 2 was examined using a Pyruvate Kinase Activity Assay kit (Sigma-Aldrich) after 2-hour stimulation by 1 μM ionomycin. All procedures were performed according to the manufacturer's instructions.

Transfection of overexpression vectors. For hCaMK4 overexpression, Flag-tagged hCaMK4–overexpressing vector generated previously was used in this study (13). For hPKM2 overexpression, the 6×His-tagged hPKM2 overexpression vector was made by Genescript. For 6×His-eGFP overexpression, pCMV-GFP was a gift from Connie Cepko (Addgene plasmid 11153) and was constructed by using the same vector as the 6×His-tagged hPKM2 overexpression vector (33). For Flag-tagged mouse CaMK4 (mCaMK4) overexpression

experiments in murine primary T cells, a previously generated vector was used in this study (13). For mPKM2 overexpression, a 6×His-tagged mPKM2 overexpression vector was made by Genescript and was constructed by using the pIRES2-DsRed-Express vector. All constructs were verified by DNA sequencing. For hCaMK4 overexpression experiments in HEK293T cells, these cells were transfected either with plasmid encoding Flag-tagged hCamK4, or mock plasmid, using Lipofectamine reagent (Thermo Fisher Scientific). For mCaMK4 and mPKM2 overexpression experiments in murine primary T cells, cells were harvested 1 day after starting culture, and empty vector, mCaMK4, or mPKM2 overexpression plasmid was transfected using the Amaxa Mouse T Cell Nucleofector Kit with the X-001 program (Amaxa) as previously described (11). The efficiency of the transfection in primary T cells was tested by flow cytometry and always exceeded 10%.

Pull-down assay. On day 2, lysates were prepared from trypsinized HEK293T cells, which had been transfected either with plasmid encoding Flag-tagged hCamK4 or mock plasmid, using a detergent-based lysis buffer. Briefly, buffer containing 50 mM Tris (pH 8), 150 mM NaCl, 1% NP-40 and a mixture of protease inhibitors (Roche Diagnostics) were incubated with cultured cells on ice, at 20 μl/mg wet cell pellet. Soluble protein extracts were clarified by high-speed centrifugation, and supernatants were incubated with anti-Flag Ab (Sigma-Aldrich) bound to Protein G Sepharose beads (Amersham). Pull-down assay was performed by binding 4 μg of anti-Flag Ab to Protein G–Sepharose (Amersham Biosciences) as previously described (34). Immunoglobulin (Ig) was cross-linked at room temperature to Protein G–Sepharose beads with 13 mg/ml dimethyl pimelimidate (Sigma-Aldrich) dissolved in 0.2 M triethanolamine and PBS (pH 8). The reaction was quenched with a 10-fold higher volume of 50 mM ethanolamine in PBS. Non–cross-linked Ab was removed with 0.1 M glycine (pH 2.5). HEK293T cell homogenates were clarified by high-speed centrifugation, and supernatants were incubated with bead-bound Ig. Beads were washed, and bound antigen was eluted with 0.1 M glycine (pH 2.5). Eluted protein was subjected to electrophoresis and visualized by Coomassie Blue staining. Coomassie gel staining was performed with a commercially available set of reagents (Invitrogen), compatible with subsequent MS, according to the manufacturer's recommendation.

Tryptic digestion and analysis by electrospray tandem MS (MS/MS). In-gel and in-solution tryptic digestion was performed essentially as described previously (35). The samples were subjected to a nano-flow liquid chromatography (LC) system. The LC system was directly coupled to a quadrupole time-of-flight micro tandem mass spectrometer at the Beth Israel Mass Spectrometry Core Facility. MS/MS data were processed and searched against the National Center for Biotechnology Information UniProt human nonredundant database (http://uniprot.org/downloads) via a Mascot search engine by using MaxQuant software v1.3.0.5 (http://www.maxquant.org) or Scaffold Q+S software (35, 36). CaMK4- or control-associated proteins were identified by MS.

Flag-tagged CaMK4/6×His-tagged PKM2 cotransfection assay. HEK293T cells were cotransfected with 4 μg of Flag-tagged hCaMK4 plasmid together with of 4 μg of 6×His-tagged hPKM2 plasmid or 6×His-tagged EGFP. Those vectors were transfected into 40% confluent HEK293T cells by polyethylenimine Max (Polycycles, Inc.) according the manufacturer's protocol.

Co-IP. After Flag-tagged CaMK4/6×His-tagged PKM2 cotransfection, cells were harvested in 1% NP40 lysis buffer. Co-IP was performed with the Dynabeads Protein G Immunoprecipitation Kit (Life Technologies) according to the manufacturer's protocol. Briefly, cell lysates were prepared as described above, and proteins were immunoprecipitated by incubation of lysates with 4 μg anti-Flag Ab (M2, Sigma-Aldrich), anti-6×His Ab (4E3D10H2/E3, Thermo Fisher Scientific), or control IgG (sc-3877 or sc2025, Santa Cruz Biotechnology) overnight at 4°C and Ab-protein precipitates were pulled down with Dynabeads Protein G. Beads were washed extensively, and proteins were eluted with the elution buffer. The presence of immunocomplexed proteins was determined by Western blotting with anti-Flag Ab and anti-6×His Ab.

Generation of lentiviral particles containing shRNAs. MISSION pLKO.1-puro empty vector control plasmid DNA (Sigma-Aldrich) was used for this subcloning. We designed 2 mouse *Pkm2*-shRNAs as listed below and subcloned them into the empty vector following the manufacturer's protocols. The following oligonucleotide sequences were used for this subcloning: 5′-CCGGCATCTACCACTTGCAGCTATTCTCGAGAATAGCTGCAAGTGGTAGATGTTTTTG-3′ and 5′-AATTCAAAAACATCTACCACTTGCAGCTATTCTCGAGAATAGCTGCAAGTGGTAGATG-3′ for *Pdp2*-shRNA1, and 5′-CCGGATCTACCACTTGCAGCTATTCCTCGAGGAATAGCTGCAAGTGGTAGATTTTTTG-3′ and 5′-AATTCAAAAAATCTACCACTTGCAGCTATTCCTCGAGGAATAGCTGCAAGTGGTAGAT-3′ for *Pkm2*-shRNA2. Sequences of cloned vectors were verified (Genewiz). MISSION pLKO.1-puro Non–Mammalian

shRNA Control Plasmid DNA (Sigma-Aldrich) was used for control shRNA. Those vectors were transfected into 40% confluent HEK293T cells by polyethylenimine Max according the manufacturer's protocol. Culture media with shRNA-containing lentiviral particles were collected on day 3 and 4.

EAE. On day 0, 8-week-old mice were immunized subcutaneously with 100 μg MOG35-55 peptide emulsified in complete Freund's adjuvant (Sigma-Aldrich) containing 4 mg/ml *Mycobacterium tuberculosis* extract (H37Ra; Difco), distributed between the 2 hind flanks. On days 0 and 2, 100 ng/mouse pertussis toxin (List Biological Laboratories) was given by intraperitoneal injection. Mice were monitored and weighed daily until day 21 of the experiment. Shikonin (40 μg/body, dissolved in 0.25% DMSO) or 0.25% DMSO in 200 μl PBS was administered twice a week intraperitoneally. The following clinical scores were used: 1, limp tail; 2, hind-limb paresis; 3, hind-limb paralysis; 4, tetraplegia; 5, moribund (37).

Adaptive transfer EAE using PKM2 inhibitor. Naive $CD4^+$ T cells from 2D2 mice were cultured with 20 μg/ml MOG35-55, 1×10^6 mitomycin-treated splenocytes, and 0.5 ng/ml rIL-12 for 48 hours as previously described (38, 39) and 0.1 μM shikonin or the same concentration of DMSO was added on day 0. Cultured cells were harvested on day 2 of culture. Five million cells were suspended in 150 μl of PBS (pH 7.4) and injected intravenously into each *Rag1*-deficient mouse. Pertussis toxin (300 ng per mouse; List Biological Laboratories) was intraperitoneally injected later on the day of transfer and 2 days later. Mice were monitored and weighed as previously described (11).

Adaptive transfer EAE using shRNA. Naive $CD4^+$ T cells from 2D2 mice were cultured under Th17 cell conditions. On day 1 of culture, *Pkm2*-shRNA– or control shRNA–containing lentiviral particles were added to the media with polybrene infection/transfection reagent (Sigma-Aldrich). One day after infection, puromycin was added to the media. Cultured cells were harvested and purified on day 4 of culture. Five million cells were suspended in 150 μl of PBS (pH 7.4) and were injected intravenously into each *Rag1*-deficient mouse. Pertussis toxin (300 ng per mouse; List Biological Laboratories) was intraperitoneally injected later on the day of transfer and 2 days later. Mice were monitored and weighed as previously described (11).

Histological staining and analysis. Sections from 10% formalin-fixed spinal cords were stained with H&E. Spinal cord sections were scored as previously described (11).

Statistics. Statistical analyses were performed in GraphPad Prism version 6.0 software. Statistical significance was determined by 2-tailed *t* test for 2 groups or 1-way ANOVA with Bonferroni's multiple-comparisons test for 3 or more groups. For the EAE experiments, clinical scores and body weight changes of each treatment group were compared using 2-way ANOVA. *P* values of <0.05 were considered statistically significant (**$P < 0.01$, *$P < 0.05$).

Study approval. All animal protocols and experiments were approved by the Institutional Animal Care and Use Committee of Beth Israel Deaconess Medical Center (no. 088-2015).

Author contributions

MK and GCT conceived and designed the study. MK, KM, ISG, WP, MU, EK, CB, SYKO, MV, MGT, and NY performed the experiments and data analysis and interpretation. MK and GCT drafted the manuscript.

Acknowledgments

This work was supported by NIH grant R01AR064350 (to GCT) and by a SENSHIN Medical Research Foundation grant (to MK), and the Japan Society for the promotion of science postdoctoral fellowships for research abroad (to NY).

Address correspondence to: George C. Tsokos or Nobuya Yoshida, Beth Israel Deaconess Medical Center, Harvard Medical School, 330 Brookline Avenue, CLS-937, Boston, Massachusetts 02215, USA. Phone: 617.735.4160; Email: gtsokos@bidmc.harvard.edu (G.C. Tsokos). Phone: 617.735.4168; Email: nyoshida@bidmc.harvard.edu. Or to: Michihito Kono, Department of Rheumatology, Endocrinology and Nephrology, Faculty of Medicine, Hokkaido University, Sapporo, Japan. Phone: 81.11.706.4638; Email: m-kono@med.hokudai.ac.jp.

1. Tsokos GC. Systemic lupus erythematosus. *N Engl J Med*. 2011;365(22):2110–2121.
2. Korn T, Bettelli E, Oukka M, Kuchroo VK. IL-17 and Th17 Cells. *Annu Rev Immunol*. 2009;27:485–517.
3. Di Cesare A, Di Meglio P, Nestle FO. The IL-23/Th17 axis in the immunopathogenesis of psoriasis. *J Invest Dermatol*. 2009;129(6):1339–1350.
4. van Hamburg JP, Tas SW. Molecular mechanisms underpinning T helper 17 cell heterogeneity and functions in rheumatoid arthritis. *J Autoimmun*. 2018;87:69–81.
5. Tang R, Langdon WY, Zhang J. Regulation of immune responses by E3 ubiquitin ligase Cbl-b [published online ahead of print November 7, 2018]. *Cell Immunol*. doi: 10.1016/j.cellimm.2018.11.002.
6. Reich DS, Lucchinetti CF, Calabresi PA. Multiple sclerosis. *N Engl J Med*. 2018;378(2):169–180.
7. Frohman EM, Racke MK, Raine CS. Multiple sclerosis--the plaque and its pathogenesis. *N Engl J Med*. 2006;354(9):942–955.
8. MacIver NJ, Michalek RD, Rathmell JC. Metabolic regulation of T lymphocytes. *Annu Rev Immunol*. 2013;31:259–283.
9. Lunt SY, Vander Heiden MG. Aerobic glycolysis: meeting the metabolic requirements of cell proliferation. *Annu Rev Cell Dev Biol*. 2011;27:441–464.
10. Kono M, et al. Pyruvate dehydrogenase phosphatase catalytic subunit 2 limits Th17 differentiation. *Proc Natl Acad Sci USA*. 2018;115(37):9288–9293.
11. Kono M, Yoshida N, Maeda K, Tsokos GC. Transcriptional factor ICER promotes glutaminolysis and the generation of Th17 cells. *Proc Natl Acad Sci USA*. 2018;115(10):2478–2483.
12. Racioppi L, Means AR. Calcium/calmodulin-dependent kinase IV in immune and inflammatory responses: novel routes for an ancient traveller. *Trends Immunol*. 2008;29(12):600–607.
13. Koga T, et al. CaMK4-dependent activation of AKT/mTOR and CREM-α underlies autoimmunity-associated Th17 imbalance. *J Clin Invest*. 2014;124(5):2234–2245.
14. Maeda K, et al. CaMK4 compromises podocyte function in autoimmune and nonautoimmune kidney disease. *J Clin Invest*. 2018;128(8):3445–3459.
15. Juang YT, et al. Systemic lupus erythematosus serum IgG increases CREM binding to the IL-2 promoter and suppresses IL-2 production through CaMKIV. *J Clin Invest*. 2005;115(4):996–1005.
16. Ichinose K, Juang YT, Crispín JC, Kis-Toth K, Tsokos GC. Suppression of autoimmunity and organ pathology in lupus-prone mice upon inhibition of calcium/calmodulin-dependent protein kinase type IV. *Arthritis Rheum*. 2011;63(2):523–529.
17. Ichinose K, et al. Cutting edge: Calcium/calmodulin-dependent protein kinase type IV is essential for mesangial cell proliferation and lupus nephritis. *J Immunol*. 2011;187(11):5500–5504.
18. Pollizzi KN, Powell JD. Integrating canonical and metabolic signalling programmes in the regulation of T cell responses. *Nat Rev Immunol*. 2014;14(7):435–446.
19. Buck MD, O'Sullivan D, Pearce EL. T cell metabolism drives immunity. *J Exp Med*. 2015;212(9):1345–1360.
20. Menk AV, et al. Early TCR signaling induces rapid aerobic glycolysis enabling distinct acute T cell effector functions. *Cell Rep*. 2018;22(6):1509–1521.
21. Park IK, Soderling TR. Activation of Ca^{2+}/calmodulin-dependent protein kinase (CaM-kinase) IV by CaM-kinase kinase in Jurkat T lymphocytes. *J Biol Chem*. 1995;270(51):30464–30469.
22. Lü S, et al. PKM2-dependent metabolic reprogramming in CD4. *J Mol Med*. 2018;96(6):585–600.
23. Chen J, Xie J, Jiang Z, Wang B, Wang Y, Hu X. Shikonin and its analogs inhibit cancer cell glycolysis by targeting tumor pyruvate kinase-M2. *Oncogene*. 2011;30(42):4297–4306.
24. Shi LZ, et al. HIF1alpha-dependent glycolytic pathway orchestrates a metabolic checkpoint for the differentiation of TH17 and Treg cells. *J Exp Med*. 2011;208(7):1367–1376.
25. Ray JP, et al. The interleukin-2-mTORc1 kinase axis defines the signaling, differentiation, and metabolism of T helper 1 and follicular B helper t cells. *Immunity*. 2015;43(4):690–702.
26. Morel L. Immunometabolism in systemic lupus erythematosus. *Nat Rev Rheumatol*. 2017;13(5):280–290.
27. Shen Y, et al. Metabolic control of the scaffold protein TKS5 in tissue-invasive, proinflammatory T cells. *Nat Immunol*. 2017;18(9):1025–1034.
28. Huang N, Perl A. Metabolism as a target for modulation in autoimmune diseases. *Trends Immunol*. 2018;39(7):562–576.
29. Yang W, et al. ERK1/2-dependent phosphorylation and nuclear translocation of PKM2 promotes the Warburg effect. *Nat Cell Biol*. 2012;14(12):1295–1304.
30. Koga T, et al. Calcium/calmodulin-dependent protein kinase 4 promotes GLUT1-dependent glycolysis in systemic lupus erythematosus. *Arthritis Rheumatol*. 2019;71(5):766–772.
31. Gao S, et al. Crosstalk of mTOR/PKM2 and STAT3/c-Myc signaling pathways regulate the energy metabolism and acidic microenvironment of gastric cancer. *J Cell Biochem*. 2018;120(2):1193–1202.
32. Yang X, et al. Pyruvate kinase M2 modulates the glycolysis of chondrocyte and extracellular matrix in osteoarthritis. *DNA Cell Biol*. 2018;37(3):271–277.
33. Matsuda T, Cepko CL. Electroporation and RNA interference in the rodent retina in vivo and in vitro. *Proc Natl Acad Sci USA*. 2004;101(1):16–22.
34. Gavanescu I, Kessler B, Ploegh H, Benoist C, Mathis D. Loss of Aire-dependent thymic expression of a peripheral tissue antigen renders it a target of autoimmunity. *Proc Natl Acad Sci USA*. 2007;104(11):4583–4587.
35. Breitkopf SB, Taveira MO, Yuan M, Wulf GM, Asara JM. Serial-omics of $P53^{-/-}$, $Brca1^{-/-}$ mouse breast tumor and normal mammary gland. *Sci Rep*. 2017;7(1):14503.
36. Breitkopf SB, Yuan M, Helenius KP, Lyssiotis CA, Asara JM. Triomics analysis of imatinib-treated myeloma cells connects kinase inhibition to RNA processing and decreased lipid biosynthesis. *Anal Chem*. 2015;87(21):10995–11006.
37. Yoshida N, et al. ICER is requisite for Th17 differentiation. *Nat Commun*. 2016;7:12993.
38. Gerriets VA, et al. Metabolic programming and PDHK1 control $CD4^+$ T cell subsets and inflammation. *J Clin Invest*. 2015;125(1):194–207.
39. Williams JL, Kithcart AP, Smith KM, Shawler T, Cox GM, Whitacre CC. Memory cells specific for myelin oligodendrocyte glycoprotein (MOG) govern the transfer of experimental autoimmune encephalomyelitis. *J Neuroimmunol*. 2011;234(1–2):84–92.